[42] N. Lagakos, R. Mohr, and O. H. El-Bayomi, "Stress optic coefficient and stress profile in optical fibers," *Appl. Opt.*, vol. 20, no. 13, pp. 2309–2313, July 1981.

✦

Ismo V. Lindell (S'68–M'70–SM'83), for a photograph and biography please see page 526 the July 1983 issue of this TRANSACTIONS.

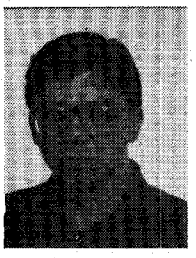

Markku I. Oksanen (S'81) was born in Jyväskylä, Finland on Dec. 1. 1958. He received the Dipl. Eng. degree in 1983 in electrical engineering from the Helsinki University of Technology, Espoo, Finland.

His main interest is in electromagnetic theory.

An Implantable Electric-Field Probe of Submillimeter Dimensions

T. E. BATCHMAN, SENIOR MEMBER, IEEE, AND GEORGE GIMPELSON, MEMBER, IEEE

Abstract—**Many areas of biological research await the development of practical electric (*E*)-field probes with submillimeter dimensions for *in situ* measurements of RF electromagnetic fields. This paper reports on the design, fabrication, and testing of such a probe. The probe consists of a 0.6-mm dipole antenna, a zero-bias Schottky barrier diode and a unique highly resistive output lead structure. Experimental results indicate the probe does not perturb the field under investigation and is linear over a range of field strengths from less than 60 to over 1200 V/m. The probe has been designed so as to be independent of the media in which measurements are being made.**

I. INTRODUCTION

IN THE MID-1970's a series of articles appeared in the *New Yorker*, written by Paul Brodeur [1], which brought to the public's attention the present controversy over the question of what constitutes a safe level of electromagnetic radiation. The debate now centers around the criteria used by the U.S. to establish an exposure limit. Initially, it was assumed that only the thermal effects were hazardous, and so all that needed to be considered was the rate at which the human body dissipated the thermal energy.

However, in the last 15 years an impressive amount of evidence has been accumulated which demonstrates the existence of "nonthermal" effects [2]–[5]. In the late 1960's, Dr. W. R. Adey (then with the Brain Research Institute of UCLA) and A. H. Frey of Randomline, Inc., advanced theories on the biological effects of very low intensity microwaves, and collected experimental evidence for theoretical verification [6]. In the early 1970's Dr. K. V. Sudakov at P. K. Anokhin Institute in Moscow induced profound EEG and behavioral changes in mice using ELF modulated microwaves. Dr. R. Carpenter of the Bureau of Radiological Health is presently attempting to determine if there is a correlation between the formation of cateracts and microwave exposure. This concern over the effects of low-level non-ionizing radiation has led to a demand for more accurate methods of measuring electromagnetic fields within biological media.

Currently, there are three methods available for determining the strength of internal electromagnetic fields: the electric (E)-field probe, thermography, and the temperature probe. A comparison of these three internal dosimetric techniques has been made by H. Bassen *et al.*, [7] and it was noted that the E-field probe measurement is the only technique which directly monitors the electric field. Consequently, it neither depends on observed secondary effects nor assumes that all the internally deposited energy is transformed to heat. Both the temperature probe and thermography require a knowledge of the mass density and specific heat of the investigated region to determine the specific absorption rate. Furthermore, the sensitivity of these two methods is not great enough to allow for dosimetry at incident power densities of less than 10 mW/cm^2, as is often needed for low-intensity microwave research. The E-field probe does not suffer from these limitations, and has the advantage of continuous line scan capability and media independence.

Manuscript received February 7, 1983; revised May 4, 1983. This work was supported by the National Science Foundation.

T. E. Batchman is with the Department of Electrical Engineering, University of Virginia, Charlottesville, VA.

G. Gimpelson is with Harris Semiconductor, Melbourne, FL.

0018-9480/83/0900-0745$01.00 ©1983 IEEE

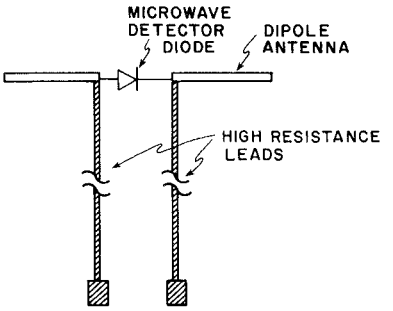

Fig. 1. Structure of the miniature E-field probe of Bassen *et al.*

Discussions and proposals for E-field probes have appeared in the literature throughout the last decade [8]–[10]. A miniature broad-band E-field probe was developed by Bassen *et al.* [11]. In this design, a diode is connected across the dipole antenna (3-mm length) and the detected signal is transmitted to an amplifier via a pair of coplanar, parallel high-resistance leads (120 Ω/□) as shown in Fig. 1. The most undesirable feature of this device was that a forward bias was required for optimum low-level performance of the microwave detector diode. Due to the added complexity of the dc preamplifier circuitry, this forward biasing could not be incorporated into the design. Discussions of this problem with device manufacturers led to development of a zero-bias Schottky barrier diode [11].

The leads of Fig. 1 are of high resistivity to reduce RF pickup. Further, it has been shown, [11], that this high impedance combined with interlead capacitance creates a low-pass filter which removes the ac from the signal detected with the diode, and also shorts the undesired lead signal. Reducing the spacing between leads is important not only to increase interlead capacitance but also to minimize the size of the magnetic loop formed by the leads.

Later probe designs employed higher resistance leads (> 250 Ω/□) and shorter dipole antennas (1.5 mm) [12]. Three of these new probes were also combined in an *I*-beam structure for measurement of the three vector field components [13].

II. The Theory and Design of the Implantable Probe

Fig. 2 shows the probe designed and fabricated by the authors for *in situ* measurements. This E-field detector is small enough (< 0.6 mm) to allow for measurements in biological media without significantly disturbing the electrical field under investigation or destroying the physical integrity of the biological tissue [7]. The smaller probe also allows for measurements closer to dielectric interfaces (0.3 mm) without significant field distortion. King and Smith have shown that the antenna must be no closer to the interface than one half the dipole length, in order to maintain a measurement error of one percent or less [14].

The beam leads of a Hewlett-Packard (HP 5082-2264) Schottky barrier diode have been reduced in width to form the dipole antenna. This diode has a cutoff frequency of 18 GHz so that detection of frequencies ranging from a few

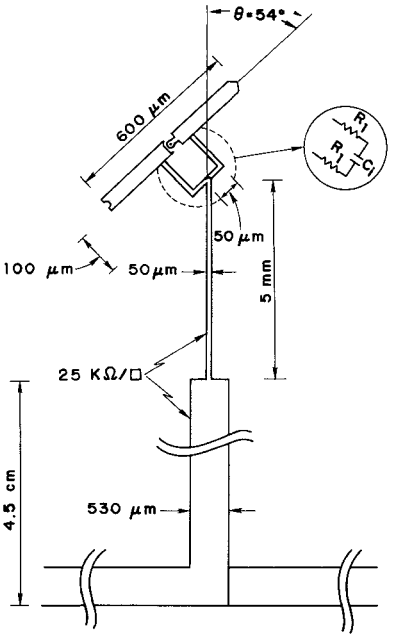

Fig. 2. E-field probe design with overlayed lead structure.

hundred megahertz to the cutoff frequency is possible with reasonable sensitivity. The unique lead structure, where the interlead distance has been minimized by overlaying the leads, is a design innovation of this probe and allows for precise control of interlead capacitance.

Detailed design of the E-field probe was accomplished by combining the equivalent circuits of the antenna, diode, and leads. The Schottky barrier diode is modeled as a resistance R_s in series with the parallel combination of the video resistance R_v and the junction capacitance C_j, as shown in Fig. 3 [15]. The short dipole antenna equivalent circuit is modeled as a current source in parallel with an admittance Y_{ant}, shown in Fig. 4(a). Smith [16] has shown that the antenna admittance can be expressed as

$$Y_{\text{ant}} = \frac{j\omega\epsilon_0\epsilon_{ei}\pi h}{\ln(b/a)} \tag{1}$$

if the condition $\gamma/[2(1+\gamma)^{1/2}] \ll 1$ is satisfied, where

$$\gamma = \frac{\epsilon_{ei}\ln(h/b)-1}{\epsilon_e\ln(b/a)} \tag{2}$$

and the symbols are defined in Fig. 4(b). As can be seen, (1) is independent of the relative permittivity ϵ_e of the biological medium, and the antenna admittance is thus unaffected by the medium in which the probe is immersed. The above criteria can be fulfilled by making the relative permittivity of the insulation ϵ_{ei} less than ϵ_e. It has been assumed in the design of this probe that

$$\gamma \simeq \frac{\epsilon_{ei}}{\epsilon_e}. \tag{3}$$

If the relative permittivity of the dipole insulation is ≤ 0.5 ϵ_e, then

$$\gamma/\left[2(1+\gamma)^{1/2}\right] \leq 0.2 \tag{4}$$

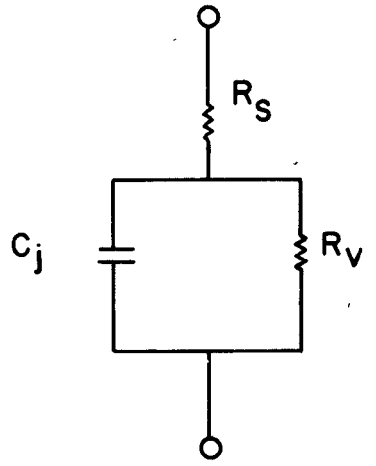

Fig. 3. Microwave equivalent circuit for a Schottky barrier diode.

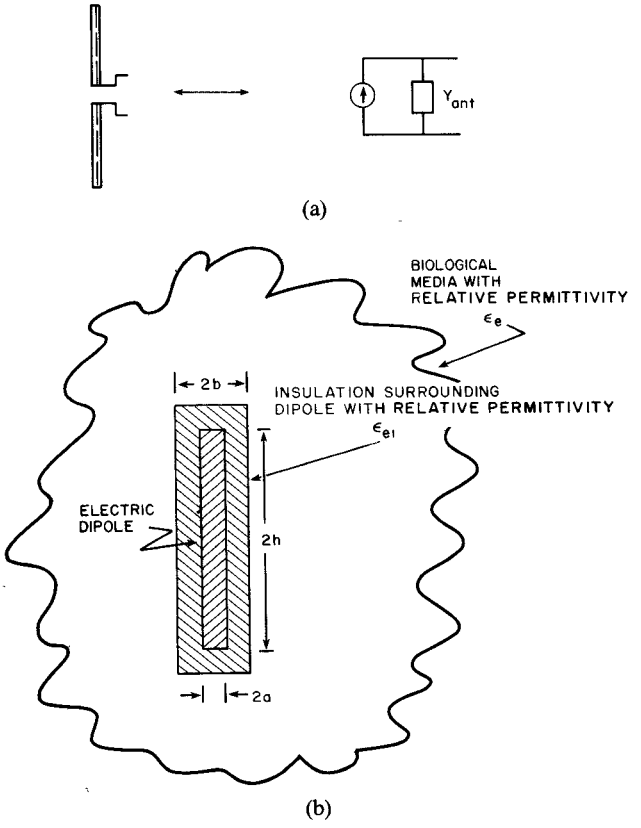

Fig. 4 (a) Short dipole antenna and its equivalent circuit model. (b) Insulated short dipole antenna immersed in a dielectric medium.

and (1) will hold. Choosing an insulating material with $\epsilon_{ei} \leq 4$ allows all media with a relative permittivity greater than 8 ($\epsilon_e \geq 8$) to be probed. Biological specimens are composed of tissue or media having relative permittivity between 5 and 100, so that most biological samples can be investigated.

The total E-field probe can be modeled as shown in Fig. 5 [14]. This circuit is divided into a high-frequency side and a low-frequency output side. In constructing the high-frequency side, it has been assumed that the series resistance of the diode R_s is much smaller than $(1/\omega C_j)$ or R_v and, therefore, can be neglected. The current produced by

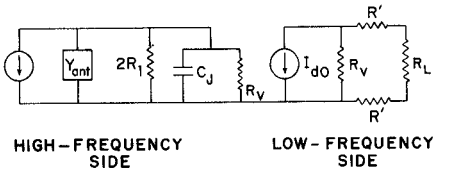

Fig. 5. Equivalent circuit model for the entire E-field probe.

the generator on the low-frequency output side I_{d0} is proportional to the amount of power dissipated by the diode. The total dc resistance of the leads is R' and the load resistance is R_L. From this model, design values for components of the probe can be calculated.

Assuming the frequency of operation is 300 MHz, the antenna admittance is approximately 3×10^{-5} S for a b/a ratio ~ 10. R_1 should be selected to force as much current as possible through the detector diode. Typical values of C_j and R_v are 0.1 pF and 300 kΩ, respectively, for a HP 5082-2264 diode at zero bias. Detector current can be maximized by satisfying the inequality

$$2R_1 \gg R_v \| 1/\omega c_j \| 1/Y_{\text{ant}} \tag{5}$$

which gives $R_1 \gg 2500\ \Omega$ for the present design. The "||" symbol indicates the parallel combination of the stated impedances. Using the dimensions for R_1 shown in Fig. 2 and choosing the value of R_1 to be 50 kΩ, the lead resistance is calculated as ~ 25 kΩ/□.

In order to guarantee that the interlead capacitance acts as a short, the impedance of the leads R_1 must be much greater than the impedance of the interlead capacitance C_i

$$2R_1 \gg 1/\omega C_i$$
$$C_i \gg 0.03\ \text{pF}. \tag{6}$$

Assuming that the microwave signal will be shorted by the first fifty micrometers (the first square) of the overlapping leads, the dielectric thickness can be calculated

$$C_i = \frac{A\epsilon_r\epsilon_0}{\tau} \gg 0.03\ \text{pF}$$
$$A = \text{area of the first square}$$
$$\tau \ll 3\ \mu\text{m}. \tag{7}$$

To reduce the probability of a breakdown in the oxide, a relatively thick dielectric layer is selected ($\tau = 1\ \mu$m).

The output leads were limited to a total resistance of between 1 and 10 MΩ, in order to be compatible with the existing preamplifier used by Bassen [13]. In addition, a lead length (l) of ~ 5 cm is desired for most measurements. Using a lead width of 50 μm and a resistance of 25 kΩ/□ results in a lead resistance of more than 25 MΩ. In order to bring this value to within acceptable bounds, the lead width is flaired out to 530 μm after the first 5 mm (see Fig. 2). A lead resistance of less than 6 MΩ can be achieved with the addition of this flaired section.

As noted earlier it is necessary to minimize the microwave signal pickup by the high-resistance output leads so that it is insignificant when compared to the signal received by the 0.6-mm dipole antenna. The distortion of the output

signal due to the lead pickup can be characterized by the parameter χ [17]

$$\chi = \frac{\ln(h/a)-1}{\pi}(\tau/h)(\zeta/2rh) \tag{8}$$

where r is the resistance of the leads per unit length, ζ is the free-space impedance, and the other symbols are as previously defined. χ is the ratio of the maximum undesired received signal to the maximum desired signal. For this probe design χ is 1.8×10^{-5}, so the lead pickup is insignificant.

In addition to minimum lead reception, the leads should not scatter a significant portion of the incident wave. The scattering cross section is defined as the time-average power scattered divided by the time-averaged power density of the incident wave. For electrically short lead structures ($\beta_0 l \ll 1$) the maximum scattering cross section σ_L is approximated by [17]

$$\sigma_L \approx \frac{2(\beta_0 l)^2}{3\pi}\left(\frac{\zeta}{r}\right)^2 \tag{9}$$

where β_0 is the propagation constant for free space ($\beta_0 = \omega/c$) and l is the total length of the high-resistance leads. For the structure under investigation, the wider section of the leads accounts for the majority of the scattering, and even this is very insignificant. At 300 MHz, $\beta_0 l$ is 0.31. Using the electrically short lead formula given above, the scattering cross section is 1.2×10^{-12} m^2. For an electrically long lead ($\beta_0 l \gg 1$), the maximum scattering cross section formula is approximately [17]

$$\sigma_L \approx \beta_0 l\left(\frac{\zeta}{r}\right)^2. \tag{10}$$

At 18 GHz, $\beta_0 l$ is 19 and the scattering cross section is still insignificant (1.1×10^{-9} m^2).

When the incident microwave field is amplitude modulated to increase the signal-to-noise ratio, the output leads form a high-resistance transmission line which acts as a low-pass filter. The passband of such a transmission line is given by

$$f_c < (4\pi C' r l^2)^{-1} \tag{11}$$

where C' is the capacitance per unit length of the output line. For the probe currently under investigation this yields $f_c < 35$ Hz. This passband is wide enough to allow for an amplitude modulated signal but narrow enough to exclude 60-Hz noise.

The final design step was to select the angle θ, shown in Fig. 2, between the antenna axis and the lead axis. Normally this would be 90°, but to facilitate the construction of a three-axis probe, a 54° angle was selected. This allows three of the same probes to be assembled in a structure having an equilateral triangle cross section that is capable of measuring the three orthogonal components of the E-field vector.

III. Fabrication of the Probe

Probe fabrication consists of three parts: production of the high-resistivity output leads, cutting down a commercially available beam lead diode to form the dipole structure, and mounting the dipole antenna onto the high-resistivity leads.

(a)

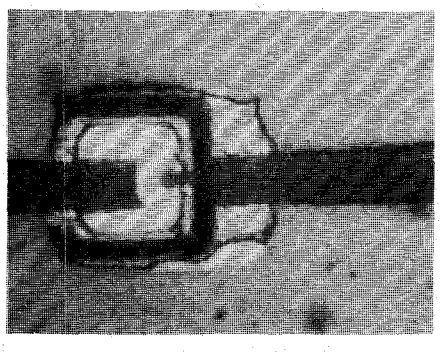

(b)

Fig. 6 (a) Unetched diode showing the center strip of photoresist and the 120-μm-wide beam leads. (b) Diode with beam leads etched to half their original width.

To simplify the probe production procedure, the beam leads of a commercially available diode have been used to form the dipole antenna elements. In order to improve directionality and to reduce nonaxial currents, a length-to-width ratio of at least ten-to-one is desirable. This has been accomplished by using standard photolithographic techniques and an exceptionally thick layer of photoresist (> 4 μm), which was needed because the beam leads to be etched were over 25 μm thick. Fig. 6(a) shows an unetched diode coated along the center with a strip of photoresist and mounted for support on a glass substrate using wax. A diode after the beam leads have been etched to one half their original width is shown in Fig. 6(b).

The lead fabrication techniques used are similar to those employed by the integrated circuit industry. A thin Ni/SiO_2 layer (~ 0.1 μm) having a resistivity of 25 k$\Omega/\square$ is sputtered onto a quartz substrate ($\epsilon_r = 4.0$). The bottom lead pattern is defined using photolithography, and then a 1-μm silicon dioxide layer is sputtered over it. A second Ni/SiO_2 film is sputtered onto the silicon dioxide dielectric. The top lead is defined using photolithography and aligned directly above the bottom lead (Fig. 7).

The tips of the leads are electroplated with gold and then an indium solder reflow technique is used to attach the dipole/diode combination. Since bonding to the leads occurs within 30 μm of the junction area, precise control of the bonding material is necessary to prevent contamination of the junction or distortion of the antenna geometry. The

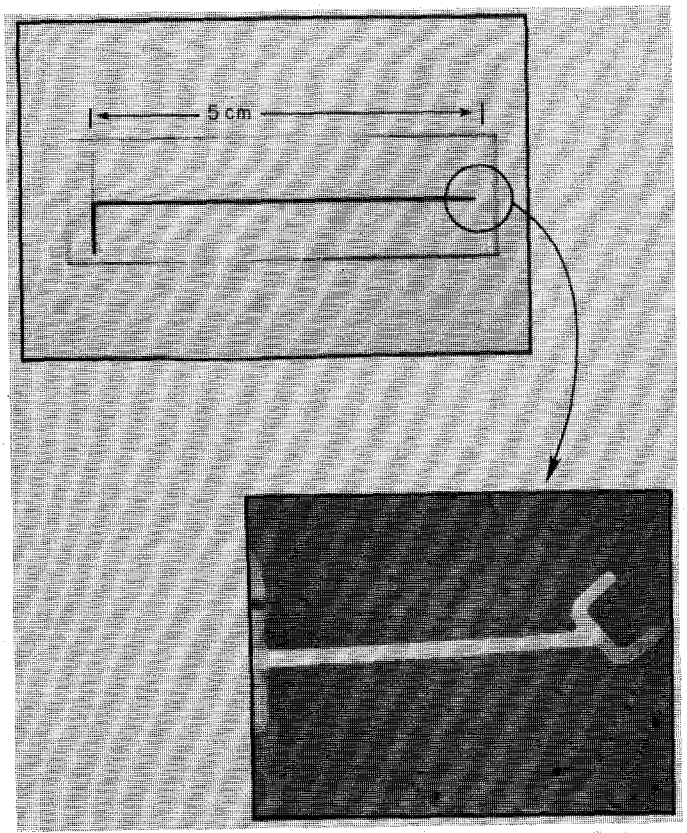

Fig. 7. Highly resistive overlayed output lead structure with magnified view of diode contact point.

solder reflow technique has proven superior to epoxy bonding in meeting these requirements.

Finally, the end of the lead structure, including the dipole, is coated with a low-dielectric-constant epoxy ($\epsilon_r < 3$) for both media independence and protection of the delicate antenna structure.

IV. Experimental Evaluation of the Probe

The probe design presented here has been fabricated, and is currently being experimentally evaluated. This includes measuring the response of the probe to an amplitude modulated signal, the dc voltage response as a function of CW signal intensity, and the output of the probe versus the angle of the incident microwave radiation.

The response of the probe to an amplitude modulated 2450-MHz signal is shown in Fig. 8. The maximum amplitude of the field incident upon the probe remained constant while the frequency of modulation was varied from 1 to 100 Hz. The amplitude of the modulated probe output signal is plotted as a function of the modulation frequency. The frequency at which the amplitude drops to 0.707 of the maximum is ~30 Hz. This is very close to the value calculated previously.

In Fig. 9(a), the dc voltage output of the probe is plotted as a function of the power density of the incident CW radiation. The E-field of the incident wave lies in the plane of the antenna and is perpendicular to the long lead axis. Since the field is at a 36° angle with respect to the dipole antenna, the measurement does not indicate the maximum sensitivity. This figure shows that the probe is sensitive

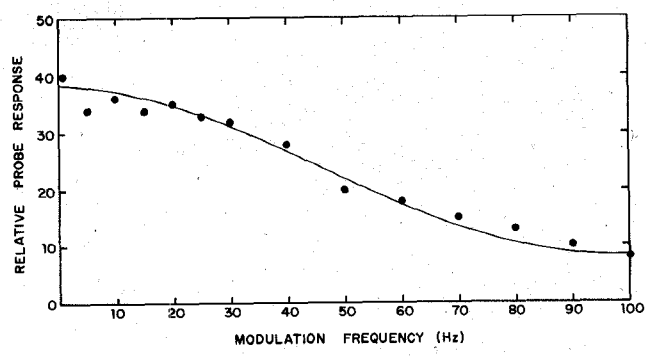

Fig. 8. Response of the probe to an amplitude modulated 2450-MHz signal.

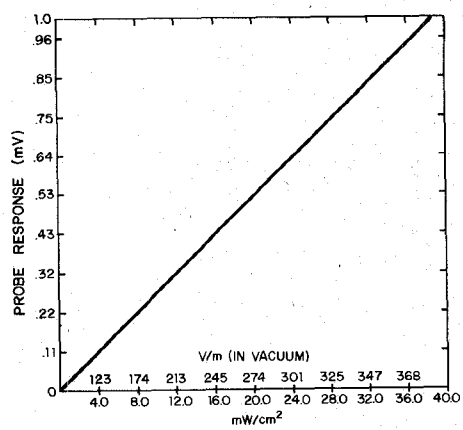

(a)

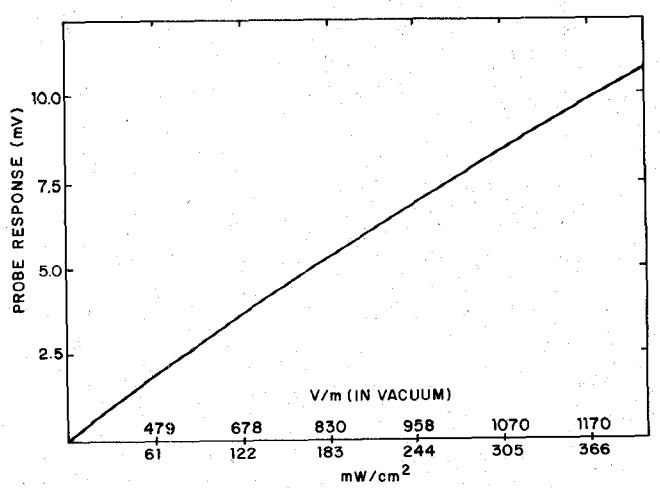

(b)

Fig. 9. The dc voltage output of the probe versus the power density of the CW radiation for (a) power densities less than 40 mW/cm and (b) power densities less than 400 mW/cm^2.

enough to allow for measurements far below the needed 10 mW/cm^2 cited in the introduction. Fig. 9(b) demonstrates that good linearity is maintained to power densities of greater than 300 mW/cm^2. Earlier probes, such as the one pioneered by Bassen *et al.*, have a response which becomes nonlinear at power densities greater than 30 mW/cm^2 [13].

Fig. 10 illustrates the experimental arrangement used to measure the antenna patterns of the probe. The incident wave has the E-field in the plane of the paper, and measurements were made at 2450 and 915 MHz. The response

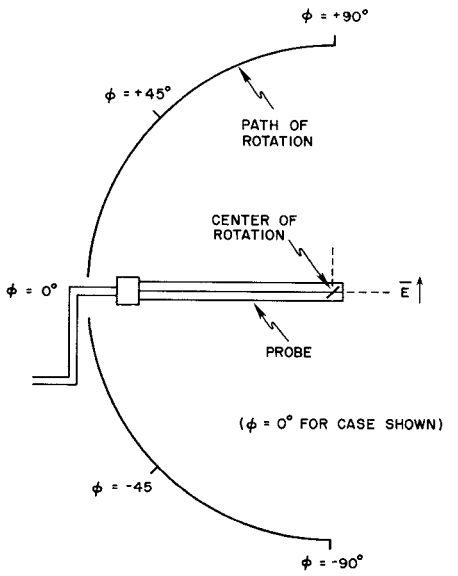

Fig. 10. Experimental arrangement used to obtain the antenna pattern of the probe.

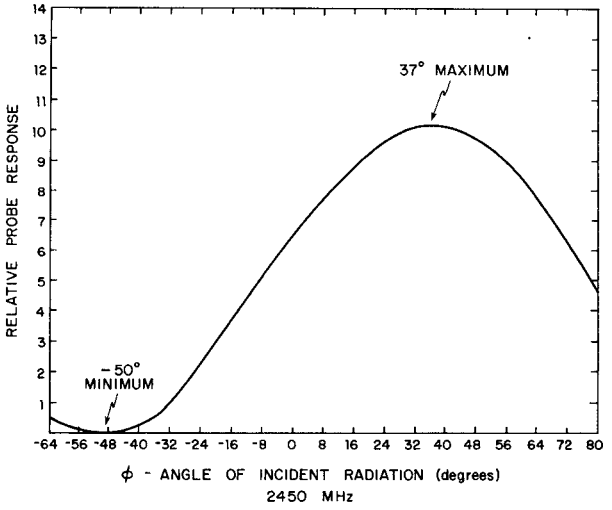

Fig. 11. Antenna pattern for 2450 MHz.

of the probe is plotted as a function of the angle (ϕ) between the direction of propagation of the incident radiation and the long output transmission line of the probe. (ϕ equals zero for the case shown in Fig. 10.)

The relative responses of the probe as a function of the angle ϕ for 2450 and 915 MHz are shown in Figs. 11 and 12, respectively. Since an accurate angular calibration was not available on the experimental measurement facility, the values of the maxima and minima angles shown on Figs. 11 and 12 may be in error and may explain differences in the predicted maximum and minimum angles compared to the measured values. In both figures the maximum should occur at 36°, and the minimum should occur at $-54°$. All angular measurements were made by establishing a reference angle by visual alignment of the axis of the probe leads with the radiation axis of the transmitting antenna. This was not a precise alignment procedure, and thus the apparent location of the maxima and minima would vary

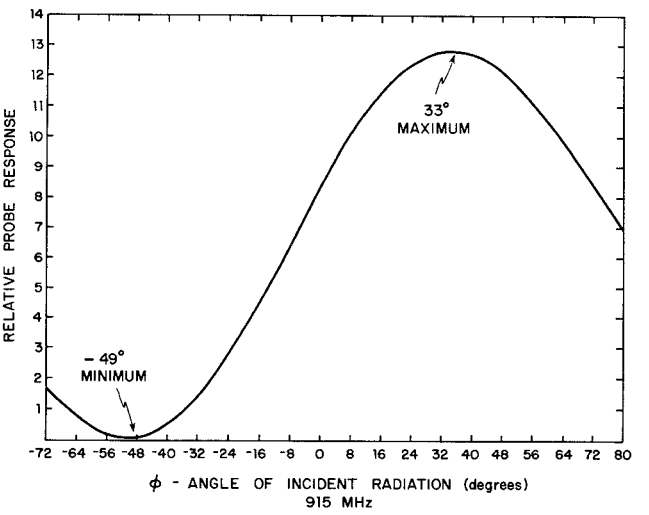

Fig. 12. Antenna pattern for 915 MHz.

between sets of measurements. Angles were then determined on the plot using this reference angle and the angular scan rate.

A second source of error arises due to the placement of the antenna with respect to the lead axis. This angle was not accurately controlled during the fabrication of the first three probes used in these measurements. An optical alignment technique is currently being utilized in fabricating the next generation of probes, and this angle error should be reduced. Other sources of error include anechoic chamber reflections and mechanical scan instability. Two characteristics of these curves should be noted. The shape of the curves are sinusoidal, indicating that the field is not significantly disturbed by the presence of the probe. Secondly, it should be realized that the minima of the curves fall to nearly the zero level of response, indicating that the leads are not acting as antennas.

V. Conclusions

The design and fabrication techniques used in constructing an E-field probe of submillimeter dimensions have been discussed in this paper. Test results from measurements on the first three probes indicate performance characteristics which verify the predicted probe bandwidth, antenna pattern, and linearity. Measurements indicate that the probe does not suffer significant noise degradation due to the extremely short dipole antenna. In a forthcoming paper, a theoretical analysis will be used to develop expressions governing both the minimum detectable signals and the upper limit to the linear output region of the probe for higher E-fields. It will be shown that shorter dipoles extend the linearity by not saturating until larger E-fields. However, as might be expected, the sensitivity is also reduced. This can be compensated for, by decreasing the passband of the output leads and judicious selecting a diode with the proper characteristics.

The good agreement between the measured antenna pattern shape and that predicted for an ideal dipole antenna is attributed to the unique output lead structure

design. This lead structure has been fabricated with a resistivity 20 times greater than that used in previous probes thus improving its transparency to microwave radiation. The overlay structure employed in the lead design increases interlead capacitance by a factor of 400 over previous designs and thus decreases distortion due to both lead E-field and magnetic loop reception.

It has been demonstrated with this probe design that it is possible to fabricate a submillimeter probe with sufficient sensitivity to be used for *in situ* biological measurements. Due to the small size of the probe and the possibility of developing even smaller probes, it now appears feasible to measure three-dimensional *in situ* fields in RF bioeffects research. Such a probe may also find application in diathermy treatment of tumors in humans as well as industrial uses in measuring field intensities in waveguides, microwave oven leakage, and RFI measurements in electronics packages.

ACKNOWLEDGMENT

The authors wish to thank H. Bassen and K. Franke of the Bureau of Radiological Health for their technical assistance and the use of the microwave measurement facility. G. Smith of Georgia Institute of Technology participated in the initial design of the probe, and has contributed to subsequent design discussions. R. Kot developed the solder reflow technique used and P. Hoeffer constructed the support fixtures for handling and testing the probe.

REFERENCES

[1] P. Brodeur, "Reporter at large," *New Yorker*, pp. 43–83, Dec. 20, 1976.
[2] P. Harris, Ed., "Effects of non-ionizing radiation given priority status by Congress," *Microwaves*, vol. 16, no. 8, pp. 9–10, Aug. 1977.
[3] N. H. Steneck *et al.*, "The origins of U.S. safety standards for microwave radiation," *Science*, vol. 208, pp. 1230–1237, June 13, 1980.
[4] S. Baranski and P. Czerski, *Biological Effects of Electromagnetic Radiation*. New York: New York University Press, 1976.
[5] S. Cleary, "Biological effects of microwave and radio-frequency radiation," *CRC Critical Rev. in Environ. Control*, vol. 7, pp. 121–166, 1977.
[6] E. J. Lerner, "RF radiation: biological effects," *IEEE Spectrum*, vol. 17, no. 12, pp. 51–59, Dec. 1980.
[7] H. Bassen, P. Herchenroeder, A. Cheung, and S. Neuder, "Evaluation of an implantable electric field probe in finite, simulated tissue," *Radio, Sci.*, Suppl., pp. 15–25, Nov.–Dec. 1977.
[8] C. C. Johnson and A. W. Guy, "Nonionizing electromagnetic wave effect in biological material and systems," *Proc. IEEE*, vol. 60, no. 6, pp. 696–718, June 1972.
[9] G. S. Smith and R. W. P. King, "Electric field probe in material media and their application in EMC," *IEEE Trans. Electromagn. Compat.*, vol. 17, no. 4, pp. 206–211, Apr. 1975.
[10] B. S. Guru and K. M. Chen, "Experimental and theoretical studies on electromagnetic fields induced inside finite biological bodies," *IEEE Trans. Microwave Theory Tech.*, vol. 24, no. 7, pp. 433–440, July 1976.
[11] H. Bassen, M. Swicord, and J. Abita, "A miniature broad-band electric field probe," *Annals of the New York Academy of Sciences*, vol. 247, pp. 481–493, Feb. 28, 1975.
[12] H. Bassen, "Improved implantable electric field probe developed," *Bioelectromagn. Soc. Newsletter*, Lab Notes, no. 5, p. 6, Mar. 1979.
[13] H. Bassen, W. Herman and R. Hoss, "EM Probe with fiber optic telemetry system," *Microwave J.*, vol. 20, no. 4, pp. 35–39, Apr. 1977.
[14] R. King and G. Smith, *Antennas in Matter*. Cambridge, MA: MIT Press, 1981.
[15] H. Watson, *Microwave Semiconductor Devices and Their Circuit Applications*. New York: McGraw-Hill, 1969, p. 373.
[16] G. S. Smith, "Comparison of electrically short bare and insulated probes for measuring the local radio frequency electric field in biological systems," *IEEE Trans. Biomed. Eng.*, vol. 22, no. 6, pp. 478–483, Nov. 1975.
[17] G. S. Smith, "Analysis of miniature electric field probes with resistive transmission lines," *IEEE Trans. Microwave Theory Tech.*, vol. 29, no. 11, pp. 1213–1224, Nov. 1981.

T. E. Batchman (M'66–SM'82) was born in Great Bend, KS, on March 29, 1940. He received the B.S.E.E., M.S.E.E., and Ph.D. degrees in electrical engineering from the University of Kansas, Lawrence, in 1962, 1963, and 1966, respectively.

From 1966 to 1970 he was an Engineering Scientific Specialist with LTV Missiles and Space Division. In 1970 he joined the faculty of the University of Queensland, Brisbane, Australia, as a Senior Lecturer. Among his research activities at the University of Queensland were integrated optics and dynamic modeling of telecommunications systems. Since 1975 he has been on the faculty of the Electrical Engineering Department at the University of Virginia, Charlottesville, where he is an Associate Professor. His current research activities include integrated optical devices and microwave sensors.

Dr. Batchman is a member of Eta Kappa Nu, Sigma Tau, Tau Beta Pi, and Sigma Xi.

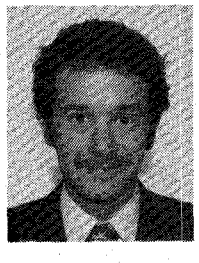

George Gimpelson (S'81–M'82) was born in Norfolk, VA, on March 3, 1955. He received the B.S. degree in physics, summa cum laude, from Hampden-Sydney College, Hampden-Sydney, VA, in 1977 and the M.S. degree in applied math and computer science from the University of Virginia, Charlottesville, in 1979. Since this time he has been pursuing his Ph.D. degree in electrical engineering at the University of Virginia. His doctoral work centers around the development of an implantable microwave probe with submillimeter dimensions.

In May of 1983, he will complete his doctoral degree and will join Harris Semiconductor in Melbourne, FL.

Mr. Gimpelson is a member of Phi Beta Kappa.